Transport in superconductor/ferromagnet/superconductor junctions dominated by interface resistance

O. Bourgeois,* P. Gandit, A. Sulpice, and J. Chaussy
Centre de Recherche sur les Très Basses Températures, Centre National de la Recherche Scientifique, Boite Postale BP 166, 38042 Grenoble, France

J. Lesueur and X. Grison
Centre de Spectrométrie Nucléaire et de Spectrométrie de Masse, Centre National de la Recherche Scientifique–Institut National de Physique Nucleaire et de Physique des Particules, Université Paris Sud, Batiment 108, 91405 Orsay, France

(Received 22 June 2000; revised manuscript received 12 September 2000; published 23 January 2001)

We report on high-sensitivity measurements performed on weakly resistive Nb/Al/Gd/Al/Nb ferromagnetic rare-earth-based junctions. High interface barriers in such junctions can strongly modify interplay between ferromagnetism and superconductivity. We show in the present paper that for such ferromagnetic/superconductor junctions that the main contribution to the resistance comes from interface scattering. On the other hand, measurements on identical nonmagnetic rare-earth-based junctions such as Nb/Al/Y/Al/Nb exhibit opposite behavior; hence most resistance comes from the bulk. A theoretical description of the temperature dependence of the superconductor/ferromagnet/superconductor ($S/F/S$) junction resistance is given through a temperature dependent Blonder-Tinkham-Klapwick theory for an energy range well below the superconducting gap scale of the Al/Nb bilayer. Such a theoretical description proves that interfacial scattering is of crucial importance when experimenting in S/F systems using gadolinium.

DOI: 10.1103/PhysRevB.63.064517 PACS number(s): 74.50.+r, 74.80.Dm, 75.70.Cn, 85.35.Ds

I. INTRODUCTION

Although the interface between magnetism and superconductivity has been studied for a long time, there has been a renewed interest in studying specific superconductor-magnetic (S-M) systems in the last few years. These studies were conducted on different devices like superconductor-ferromagnet (S-F) superlattices, superconductor/ferromagnet/superconductor ($S/F/S$) junctions, or various S-F mesoscopic systems. Very interesting results were obtained on such systems showing some new aspects of interplay between superconductivity and magnetism. In S-F superlattices, a nonmonotonic decrease of superconducting critical temperature was obtained versus the ferromagnetic thickness in the multilayer.[1–3] These observations were the first evidence of a π junction[4] using low-temperature superconductors. Also, anomalous proximity effects were obtained in S-F mesoscopic experiments, revealing unexpected superconducting long distance coherence in magnetic compounds.[5–7] Recently, important results on spin polarization at the Fermi level in magnetic compounds were found by spin-polarized experiments between a ferromagnet and a superconductor.[8,9]

More recently, Gandit *et al.*[10] proved the existence of the Josephson effect through a ferromagnetic layer in $S/F/S$ junctions. The presence of a supercurrent was the first direct evidence of superconducting coupling through a ferromagnetic layer, despite a strong pair breaking effect in the F layer. Moreover, a nonmonotonic decrease of the critical current versus the thickness of the magnetic compound was a good indication for a π coupling between both superconducting sides of the $S/F/S$ junction.[11,12]

The quality of the interface is of great importance to interpret the results in all these experiments. Indeed, several theoretical works showed the impact of interfacial resistance, especially in spin polarized experiments,[13] on the actual coupling between S and F films. Žutić and Valls[13] calculated that increasing interfacial resistance in S/F spin-polarized experiments can modify drastically the results and lead to wrong interpretations if it is not taken into account. Finally, in a recent experiment Aarts *et al.*[26] took into account the interface quality between the superconductor and the ferromagnetic compound in their sample for interpreting the results. They showed that the transparency of the S/F interface is tunable by the magnetic behavior of the F layer.

We want to stress that the knowledge of the interface quality between the superconductor and the ferromagnet is essential for a good understanding of interaction phenomena in S-F structures, such as the proximity effect, induced spin polarization, or the existence of π coupling. Numerous experiments on S-F systems are done using gadolinium (Gd) as the ferromagnetic compound, especially in critical temperature measurements in S-F superlattices.[1,2,10] Because of the well-known chemical instability of gadolinium, we decided to study by transport measurements the interfacial behavior of Gd in $S/F/S$ junctions. In this paper, we report on high-sensitivity transport measurements on Nb/Al/Gd/Al/Nb magnetic junctions and Nb/Al/Y/Al/Nb nonmagnetic junctions. Because Gd is more easily oxidized than Y, the comparison of electrical measurements in both types of junctions is of great interest to stress the difference between the contribution coming from interface quality or from bulk properties in the transport characteristics of such junctions. We then expect that transport measurements of Gd junctions are dominated by interface scattering instead of by bulk properties in Y junctions. An accurate description of the results are given using a temperature-dependent Blonder-Tinkham-Klapwijk (BTK) theory for Gd-based junctions, proving the specific behavior of interface resistances in such junctions.

In the first part of this paper we describe the sample

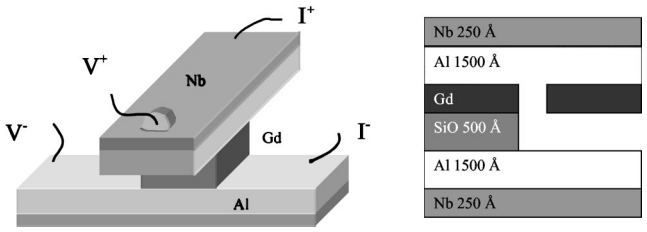

FIG. 1. Cross section of an Nb/Al/Gd/Al/Nb junction. The bias current is applied perpendicular to the layer. The SiO window defines the width of the junction 100 μm$\times$100 μm. Contacts are made on the Nb leads.

preparation and the details of the experimental setup; second, we discuss the magnetic and structural characterization of the junction; and finally we describe the results on resistance measurements and the theoretical interpretation through BTK theory.

II. EXPERIMENTAL ENVIRONMENT

A. Sample design and experimental setup

In prior work, *S-F* superlattices were studied with an applied current in the plane (CIP) of the layers. These kinds of measurements lead to information on the critical temperature of the sandwich. However, because of the uncertainty of the number of layers inspected by the measuring current, it does not give information on interface resistance or interface scattering. To do this, we designed a specific experiment on Nb/Al/Gd/Al/Nb junction with the measuring current perpendicular to the plane (CPP). Using the CPP method, we make sure that the bias current passes through all the layers without disturbing specular reflections as in CIP measurements. In these samples, the niobium layers (25 nm) are the electrodes, and contacts are made on them. We studied the interface between a 150 nm aluminum layer and a gadolinium magnetic layer with thicknesses ranging between 2 and 11 nm or a yttrium layer with a thickness of 80 nm (see Fig. 1). The Al layer is superconducting by proximity effect with the Nb layer. We used two different superconductors to separate the transition of the Nb leads and the transition of the Al/Gd/Al junction.

Because all the compounds of the junctions are metallic, measurements at very low voltage are required. For this purpose, we adapted a dc current method based on a superconducting chopper working at 4.2 K, enclosed in a dilution refrigerator to measure the sample down to 50 mK, which allows us to measure the voltage down to a picovolt with a noise of 1×10^{-14} V without magnetic field. Hence, resistance of the order of $\mu\Omega$ with current ranging between 0.1 μA and 10 mA can be easily probed. This technique was already successfully applied to very low resistance measurements on magnetic multilayers.[14] Applying this high-sensitivity device to a *S*/*F*/*S* low-resistance junction can lead to very exciting results.

The different layers are made by *e*-beam evaporation *in situ* at room temperature on a (100) silicon substrate in a UHV chamber. Using five different masks, we are able to successively evaporate Nb leads, Al, and a window of SiO to define the size of the junction as 100 μm$\times$100 μm (see Fig. 1). The evaporated thicknesses are measured by a quartz crystal microbalance and controlled *a posteriori* by Rutherford backscattering measurements, indicating a good accuracy of metallic thicknesses measured with an error of 0.25 nm.

The pressure in the UHV chamber before and during evaporation is a crucial parameter to control the quality of Al/Gd and Al/Y interfaces. We had a base pressure ranging between 10^{-9} Torr and 4×10^{-9} Torr. Gd is evaporated at a pressure around 4×10^{-9} Torr, Al and Nb with pressure of the order of 5×10^{-9} Torr, and SiO 2×10^{-8} Torr. The evaporation rate was 0.1 nm/s for Gd and 2 nm/s for Al. Low rate and low pressure are of great importance to optimize the quality of our junction.

B. Magnetic and structural characterization

Several methods were used to characterize the Gd layer. First, transmission electron microscopy (TEM) images on Al/Gd reference samples, evaporated under the same conditions as the junctions, have shown that Gd layers thinner than 2 nm are not continuous, thus imposing a lower bound on samples thicknesses, to make sure that we do not measure junctions with pinholes. Gd is polycrystalline and the size of grains ranges between 7 and 10 nm. For the smaller thicknesses, the grains are elliptic, of typical dimensions 2 nm $\times$7 nm$\times$7 nm; such a granular structure must have an impact on interface structure.

The magnetic properties of Gd were investigated by means of superconducting quantum interference device (SQUID) magnetometry. This magnetometer allows us to measure 10^{-7} emu at low field and 10^{-6} emu at high field. The magnetic field is applied in the plane of the junction. We used reference samples of size 5 mm long and 2 mm wide evaporated under the same conditions as the junctions, because the magnetic signal from the Gd inside the junction was too low to be measured directly. In Fig. 2, we show a zero-field-cooled (ZFC) and field-cooled (FC) magnetization curve in a low applied magnetic field ($H=5$ mT). This curve exhibit a large thermomagnetic hysteresis with an irreversibility temperature (T_i) of 150 K, and a blocking temperature of about 120 K. We estimate that the Curie temperature ranges between 50 K and 100 K. This behavior is characteristic of a superparamagnet, in agreement with the granularity of the magnetic layer. Thicknesses between 2 nm and 11 nm of Gd were studied, showing similar behavior. From the saturation magnetization, the magnetic moment per atom is estimated to be $4\mu_B$ for all thickness of Gd (see Table I), substantially below the Gd bulk moment of $7.6\mu_B$. We attribute this reduction of the saturation magnetization compared to the bulk value to frozen spins that do not align in the applied magnetic field due to spin glass effects as is expected for Gd small grains.[15] The eventual existence of an angle between magnetization and the applied magnetic field[16] can also lead to such reduction of magnetization. Indeed, the magnetization is not necessarily in the plane of the magnetic layer. We now have a good knowledge of the Gd layer. Above 2 nm, these layers are continuous, polycrystal-

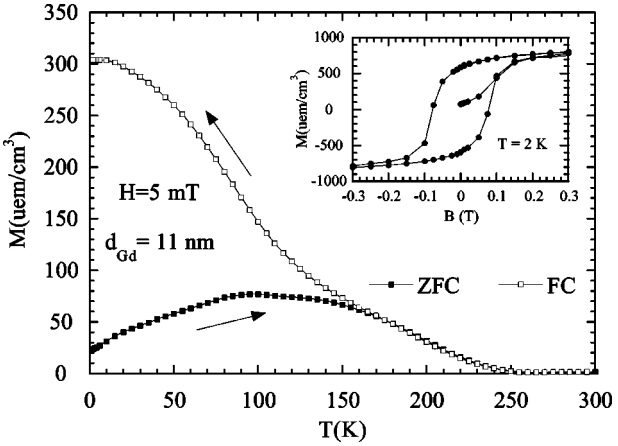

FIG. 2. Thermomagnetic hysteresis on an 11 nm Gd layer in a field of 5 mT. The full squares correspond to the ZFC curve and the open squares to the FC curve, the irreversibility temperature at 150K is clearly visible. Inset: hysteresis loop of the same sample at 2 K. The magnetic field is applied in the plane of the magnetic layer.

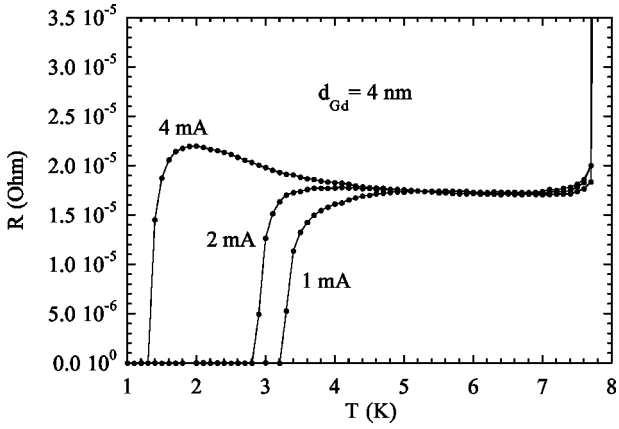

FIG. 3. Resistance versus temperature in a junction containing 4 nm of Gd with three different bias currents. Two different transition temperatures can be distinguished, one related to the junction (Gd) between 1.4 and 3.2 K depending of the bias current and one to the superconducting leads in Nb at 7.6 K.

line, and magnetic; all these characteristics will play an important role for understanding the results. In the case of yttrium, we used a large thickness of Y such that we do not expect any problems related to the layers continuity.

III. INTERFACE SCATTERING AND TRANSPORT MEASUREMENTS

A. Results

First, measurements were done to characterize the superconducting behavior of each junction. In Fig. 3, we show classical resistance versus temperature curves. For a low current measurement such as 1 mA, two different superconducting transitions can be distinguished. The transition of Nb leads at 7.6 K, and the transition of Gd at 3.2 K. The second transition is tunable with the bias current. If we use a higher current, the first transition remains at 7.2 K, but the second transition appears at lower temperature: $T_c = 2.8$ K at 2 mA and $T_c = 1.4$ K at 4 mA. This is a good indication that the second transition temperature is related to the transition of the junction, while the first transition is not affected by a changing bias current. Several different regimes can be distinguished in the $R(T)$ curve at 1 mA. First, below 3.2 K all the compounds in the junction are superconducting; a superconducting current flows through the ferromagnetic layer. Second, between 3.2 K and 7.6 K the junction is resistive. Because all the interesting interactions between the superconducting Al layer and the Gd layer appear in this resistive regime, we are going to study it carefully with temperature. Finally, all the layers including Nb are in the normal metal state above 7.6 K.

TABLE I. Magnetic moment per atom versus the Gd thickness. The values are almost constant between $3\mu_B$ and $4\mu_B$, indicating a rather homogeneous magnetic behavior in different thicknesses of Gd.

d_{Gd}	2	4	6	10	11
μ/μ_B	2.6	2.7	4.3	3.2	4

The presence of pinholes in the junction can strongly perturb our interpretation of temperature variations of resistance in the resistive regime of the junction. The study of the $S/F/S$ supercurrent (intensely studied elsewhere[10,11]) can give important information about the quality of the junction. The $V(I)$ characteristic of a junction with 6 nm of Gd at 1 K shown in Fig. 4(a) indicates that there is a well-defined critical current and a good Ohmic behavior for currents above the critical current. In order to prove that this critical current is due to a Josephson coupling, we measure oscillations of critical current with a weak applied magnetic field in the plane of the junction. Oscillations with a periodicity of 0.2 mT appear, like in classical Fraunhofer pattern, corresponding exactly to the penetration of a quantum magnetic flux (Φ_0) in the junction.[11] These measurements assure us that there is no pinhole in our junction even at low thicknesses of Gd.[17] These critical currents decrease exponentially with gadolinium thickness, leading to a penetration depth of Cooper pairs on the order of 2 nm in the range of the Gd thickness used in these junctions. Furthermore, a description using a typical resistive shunted junction (RSJ) model helps us to confirm that Gd layers are continuous inside the junctions. This model assumes that we can describe a real junction by a Josephson junction shunted by a resistor. Under this hypothesis, the voltage in the junction behaves as $V(I) = R\sqrt{I^2 - I_c^2}$.[18] The solid line in Fig. 4(a) gives the fit of the $V(I)$ characteristic of the junction with 6 nm of Gd. The excellent agreement between the model and the measurements is a second indication that these $S/F/S$ junctions behave as Josephson junctions. Hence, we can trust the resistive measurements that there will be no spurious effect due to uncontrolled structural quality of the Gd layer. By increasing the bias current we can keep the junction resistive down to low temperature, and by this way study the evolution of the resistance of such junctions in this regime. Close to the critical temperature of the ferromagnetic layer, the resistive

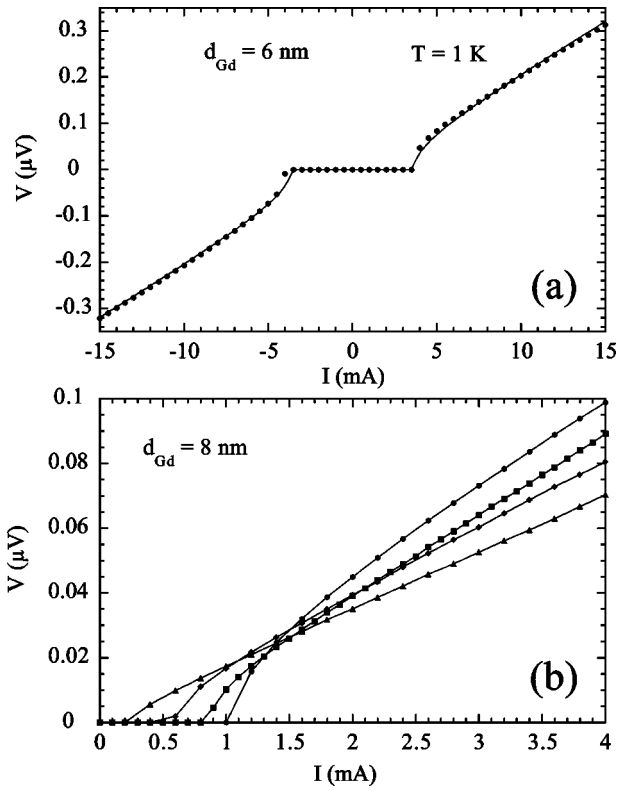

FIG. 4. $V(I)$ characteristic for two different junctions. (a) 6 nm of Gd at 1 K. The resistance of the junction is 2.2×10^{-5} Ω. The solid line corresponds to the fit using the RSJ model. Two different parameters were used: the resistance of the junction $R=2.2\times10^{-5}$ Ω and the critical current $I_c=3.65$ mA. (b) 8 nm of Gd in the junction. Measurements at four different temperatures are displayed. The critical currents are at 1 K (circles) $I_c=1$ mA; at 1.5 K (squares) $I_c=0.8$ mA; at 2 K (diamonds) $I_c=0.6$ mA; and at 3 K (triangles) $I_c=0.2$ mA.

measurement has no physical meaning, the junction being in a transient regime. But as soon as the bias current is larger by a factor of 3 than the critical current, the measured resistance is equal to the normal resistance with an accuracy of few percent following the RSJ model.[18] In the following, all resistive measurements [$R(T)$ or $R(H)$] are made with a bias current much larger than the critical current of the junctions.

In Fig. 4(b), we plot different $V(I)$ characteristics for different temperatures 1 K, 1.5 K, 2 K, and 3 K. If the temperature increases, the critical current decreases as expected in a Josephson superconductor/normal conductor/superconductor ($S/N/S$) junction, but the slope of the $V(I)$ curves is less and less steep. By performing resistance versus temperature measurements with high bias current we recover such increases of resistance at low temperature. In Fig. 5, $R(T)$ with different bias currents are shown. At 5 mA the junction has an Ohmic behavior, as controlled by $V(I)$ measurements, and a strong increase of resistance at low temperature is observed. Curves at 1.5 mA and 2 mA are in the transitory regime between Josephson and Ohmic regimes. This explains why the resistance for different bias currents are not equal. Moreover, as the measuring current is above the critical current, no superconducting transition temperature of the junction remains. We have observed such large drops of resistance with all the junctions exhibiting Josephson effect with a saturation of the increase of resistance at low temperature below 1 K. In Fig. 5, this saturation appears for the 5 mA measurement, because the bias current is much higher than the critical current of the junction. In some samples there can be a factor of 10 between low-temperature and high-temperature resistance values. Resistances range between several $\mu\Omega$ and several mΩ depending on the sample. The contribution to the resistance from the Gd bulk can be estimated to less than 10^{-6} Ω, if we assume that the resistivity of Gd at low temperature is around 140 $\mu\Omega$ cm. This estimate is orders of magnitude below what we measured in our junctions. It implies that the major contribution to the resistance comes from the interface between Nb/Al and Gd. As expected, the transport in such junctions is dominated by interfacial resistance.

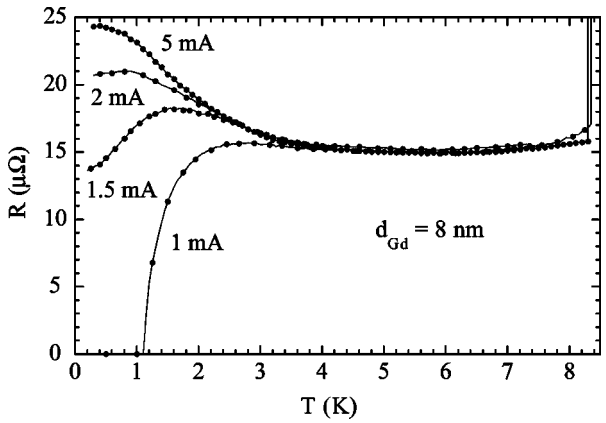

FIG. 5. Resistance versus temperature of a junction with 8 nm Gd for four different bias currents. The $R(T)$ curve at 5 mA bias current exhibits a large increase of resistance at low temperature. The increase of resistance saturates at low temperature (below 1 K).

The increase of resistance at low temperature is an unexpected phenomenon in large nonmesoscopic $S/N/S$ junctions. To the best of our knowledge, no such measurements have been reported before. It is of great interest to compare results on Gd-based junctions to the one on Y-based junctions. Because Y is a more stable nonmagnetic compound we expect better interface transparency between Al and Y. The resistance versus temperature behavior using a bias current of 20 mA on a junction containing 80 nm of Y is shown in Fig. 6. We note that the resistance decreases at low temperature. Modulation of critical current with a periodicity of 0.1 mT with a weak magnetic field shows a classical Fraunhofer pattern in $S/N/S$ junctions, confirming the existence of the Josephson effect in this junction. Because in Y no depairing process appears, the Y-based junction has a very high critical current compared to the magnetic Gd-based junctions. It was difficult to measure the resistance below 2 K. High bias currents would be needed, leading to a significant heating effect of the sample. If we assume that the resistivity of Y at low temperature is 40 $\mu\Omega$ cm, the resistance of the order of 1 $\mu\Omega$ is what we expect in the case of bulk resistive dominated behavior. Hence, if the resistance comes essentially from the bulk, no increase of resistance at low temperature is

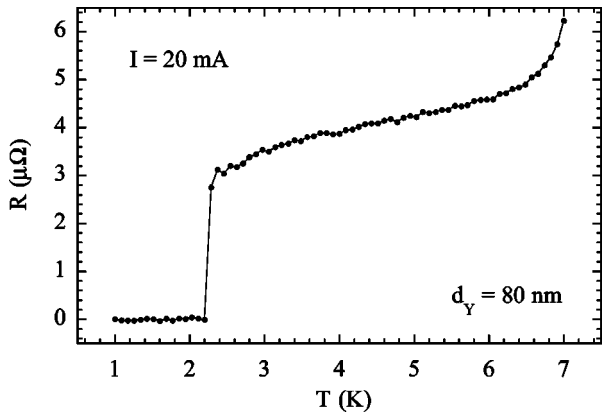

FIG. 6. Resistance versus temperature of an Nb/Al/Y/Al/Nb junction, where $d_Y = 80$ nm with a bias current of 20 mA. No increase of resistance is observed.

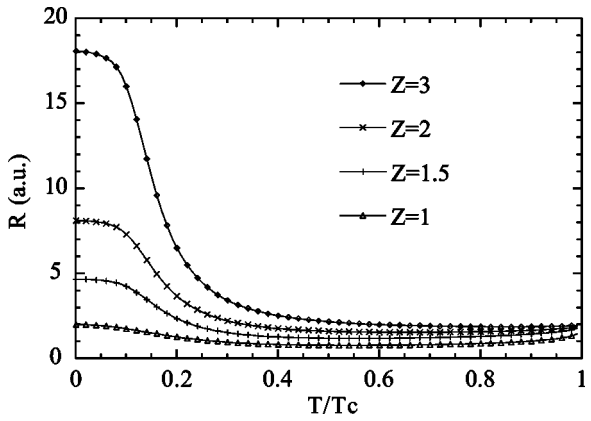

FIG. 7. Numerical simulation of resistance versus temperature in a $S/N/S$ junction, in the low-voltage regime using the BTK theory. Only resistive contacts are considered: $1 \leqslant Z \leqslant 3$. T_c is the critical temperature of the superconductor; resistances are in arbitrary units. We recover the saturation of the increase of resistance at low temperature.

observed, confirming that the increasing resistance at low temperature on Gd-based junction is directly related to interface scattering process.

B. Theoretical interpretation

The problem that arises is to clearly understand the temperature behavior of a resistive normal-metal–superconductor junction. In our samples, transport measurements were made at energy well below the order of magnitude of meV for a superconducting energy gap. Because of low-resistance samples, voltages above 1 μV were not used. In a classical N/S sandwich, the zero-temperature current is transmitted below the superconducting gap via Andreev reflections only. In the Andreev process, an incoming electron with an energy E below the superconducting gap is reflected as a hole with an energy $-E$ and an opposite wave vector, whereas a Cooper pair is transferred into the superconductor.[19] The origin of energy is taken at the Fermi level $E_F = 0$. Blonder, Tinkham, and Klapwijk[20] have shown that the Andreev reflection is weakened when the interfacial elastic process are taken into account in the form of a repulsive potential $V(x) = H\delta(x)$ localized at the interface, $x = 0$. This theory interpolates between a perfect transparent interface and an insulating barrier as the dimensionless barrier strength $Z = H/\hbar v_F$ increases from zero to infinity. This parameter is directly related to the barrier transparency T by $T = 1/(1+Z^2)$.

This model allows us to solve the Bogoliubov–de Gennes (BG) equations,[21] especially adapted to inhomogeneous systems like N/S junctions, by assuming that electronlike or holelike quasiparticles in N or S can be described by plane waves. It is allowed if the width of the junction is large compared to the Fermi wavelength, which is the case in our junction. Solving the BG equations with plane waves, we can express the current flowing through the junction by transmission coefficients, $A(E)$, which is the Andreev reflection probability coefficient, and $B(E)$, which is the probability coefficient for retroreflected electrons. Thus, the $I(V)$ characteristics can be calculated leading to the following expressions:

$$I = 2N(0)ev_F S \int_{-E_F}^{\infty} [f_0(E-eV) - f_0(E)][1 + A(E) - B(E)]dE, \tag{3.1}$$

where S is the cross section of the junction, $N(0)$ the density of states at the Fermi level, v_F the Fermi velocity, and $f_0(E)$ the Fermi distribution function, the latter two are supposed to be identical on either side of the S/N junction.

Including the temperature dependence for the superconducting gap in the Al/Nb bilayer, which is hard to calculate in the presence of the proximity effect between the Al and the Nb layer, does not improve the quality of the fit. Then for simplicity, the superconducting gap of the Al/Nb bilayer in this modelization is set constant in temperature. If we consider only perfectly transparent interfaces ($Z = 0$), this model is only valid for small junctions, i.e., a point contact with a moderate number of channels. But, for more resistive interfaces ($Z \approx 1$), we can extend this model to a larger junction like ours. Especially for high values of Z, this model correctly describes large superconductor/insulator/superconductor ($S/I/S$) junctions. Our experiment is of great interest because the Gd-based junctions are in a less-known intermediate regime between S/N low interface resistance experiments[22] and $S/I/N$ or $S/I/F$ insulator junctions.[23] By considering the low-voltage limit ($eV \ll \Delta$), we make sure that $I(V)$ characteristics calculated from Eq. (3.1) has Ohmic behavior, so we are able to calculate the junction resistance for different barrier interfaces Z. In Fig. 7, we show four $R(T)$ curves calculated from Eq. (3.1) in the low-voltage regime for different values of Z from 1 to 3. We recover a nonmonotonic behavior in temperature for the junction resistance, with a drop at low temperature.

Adjustments between experimental data and the BTK theory are given in Fig. 8 in two extreme cases of samples, one with a rather low interface resistance ($Z = 1$) and one with a high interface resistance ($Z = 2.5$). In such numerical adjustments, we consider a double-barrier junction $S/N/S$,

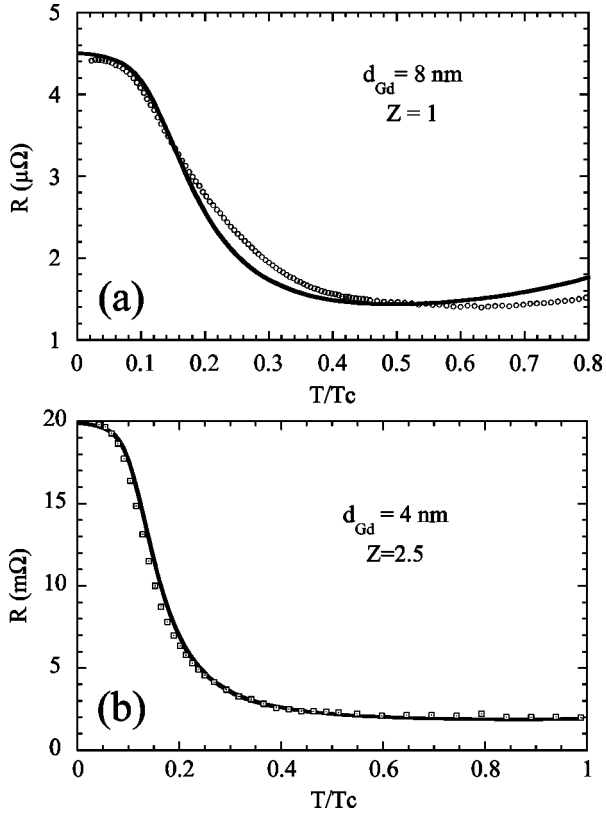

FIG. 8. Fit of the experimental resistance versus temperature curve for two different samples. (a) Low-resistance sample ($R=1.4\times10^{-6}$ Ω) with 8 nm of Gd. The measured T_c was $T_c=8.2$ K. The best fit is obtained for $Z=1$. (b) High-resistance sample ($R=2\times10^{-3}$ Ω) with 4 nm of Gd in the junction. The measured T_c was $T_c=7.5$ K. Good agreement is obtained for $Z=2.5$.

where the physics is close to the simple one-barrier model described previously. While there is good agreement between theory and experiment in the low $Z=1$ case [Fig. 8(a)], there is an excellent agreement for $Z=2.5$ [Fig. 8(b)]. For $Z=1$ the jump of resistance is of a factor of 2.5 and in the case of $Z=2.5$ the jump is a factor of 10, a significant increase of resistance. To do these fits, we only used the parameter *Z*. The agreement in the $Z=2.5$ fit is better because the junction is much more resistive and hence the BTK theory is more suitable in the case of a large junction, as we explained before. In the case of a low-resistance junction the BTK theory cannot provide a good description in the limit of our large junction. We always used $R(T)$ measurements at currents far above the critical current to be sure that the junction is largely in a constant-resistance regime. The BTK theory in the $S/N/S$ case describes correctly the increase of resistance at low temperature. It is an important confirmation that the interface scattering dominates the transport properties in such Gd-based junctions. At low temperature (below 1 K), the electron transfer is dominated by Andreev reflections. This process is strongly perturbed by scattering at the interface, which explains why the resistances are so high in case of high-*Z* barriers. At higher temperature, the decrease of resistance in such junctions is due to thermally activated electron transfer between the *N* and the *S* sides.

TABLE II. Values of the fit parameter *Z* for different thicknesses of Gd in the junction. No obvious correlation appears between the thickness of Gd and the interface potential.

d_{Gd}	4	4	6	6	8	10
Z	1.4	2.5	1.2	2	1	2

In Table II, we summarize the values of the fit parameter *Z* obtained from the adjustment of all the $R(T)$ data by plotting *Z* versus different thicknesses of Gd in the junction. No obvious correlation appears between the thickness of Gd in the junction and the value of the barrier strength *Z*. The apparent dispersion of *Z* values is due to the extreme sensitivity of the surface quality to growth parameters.

Because Gd is surrounded by a superconductor, it is possible to apply BTK theory to our sample. To prove that the drop of resistance is only related to the presence of superconductivity, we applied a strong magnetic field in the plane of the junction. By destroying superconductivity in the Al layer, we should restore the normal-metal interface behavior between Al and Gd. The electron transfer no longer involves Andreev reflections. In Fig. 9, we show the effect of magnetic field on Gd- and Y-based junctions. Opposing effects are observed. Indeed, for the Gd-based junctions [see Fig. 9(a)], the resistance decreases when applying a magnetic field because the magnetic field mimics the effect of temperature, while in the Y-based junction, applying a magnetic field increases the resistance [see Fig. 9(b)]. In this latter case, the excess of resistance comes from the Al layer switching progressively to the normal state. The characteristic field between 70 and 100 mT corresponds to the field needed to suppress superconductivity in Al layer. These additional observations confirm that the BTK theory is perfectly adapted to describe our experimental data on the Gd-based junction. On the other hand, BTK theory cannot match measurements on Y-based junctions. In such junctions, low interface resistances are present; thus low *Z* values would be necessary to fit the data. We already explained, in the case of very low interface scattering potential when the bulk resistance dominated the transport, that the BTK theory is not applicable to our large junctions.

Just considering poor interfaces due to possible damaged surfaces of the Gd layer cannot afford an explanation for such high barrier potentials in UHV evaporated junctions. Octavio *et al.* showed that if there is a Fermi wave vector mismatch (FWM) between both sides of an N/S junction,[22] an effective potential appears even if the interface is perfectly transparent. Their theory consists of renormalizing the parameter *Z* to take into account the FWM; they obtain for the effective barrier strength

$$Z_{eff}=\sqrt{Z^2+\frac{(1-r)^2}{4r}}, \tag{3.2}$$

where *Z* is the barrier strength without FWM and r is the ratio of the Fermi velocities $r=v_F^N/v_F^S$. In our case, knowing

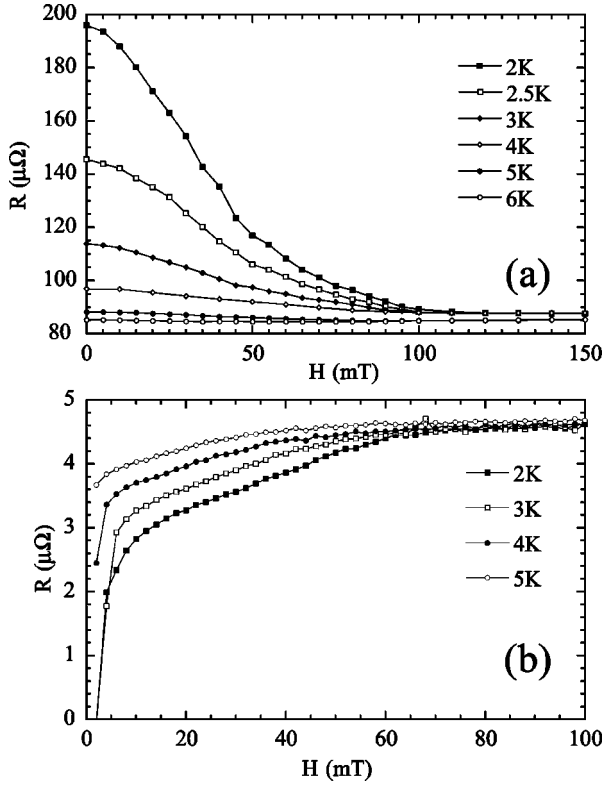

FIG. 9. $R(H)$ measurements with the magnetic field applied in the plane of the junctions. (a) Resistance versus magnetic field in an Nb/Al/Gd/Al/Nb junction for different temperatures. By destroying superconductivity we restore a classical normal metal/normal metal junction; hence the resistance of the junction at low temperature decreases. (b) Identical measurements on an Nb/Al/Y/Al/Nb junction. Application of a magnetic field increases the junction resistance.

that $v_F^{\mathrm{Gd}} \approx 5\times10^7$ cm/s and $v_F^{Al} \approx 2\times10^8$ cm/s we obtain $r = 0.25$. Hence, even if there is a perfectly transparent interface, meaning $Z=0$, there is a high effective barrier strength of $Z_{eff}=0.75$. Thus, a non-negligible part of the potential barrier can be due to FWM between Al and Gd. We believe that the other part comes from the presence of a noncontrolled damaged surface in the Gd layer, which could be due to granularity, partial oxidation of the Gd layer, or weak pollution of the Gd/Al interfaces.

We did not discuss the impact of the ferromagnetic character of Gd on the barrier potential. From recent theoretical[24] and experimental[8,9] works, we know that the presence of a spin polarization at the Fermi surface can strongly suppress Andreev reflections between the ferromagnetic side and the superconductor in an F/S junction. In a ferromagnet described by a simple Stoner model, one spin population is depleted with respect to the other. Because the incoming electron of spin σ is reflected as a hole in the opposite band of spin $-\sigma$, an Andreev reflection is allowed just to empty states in the less populated band. Even if the polarization in Gd is weak [7–15 % (Ref. 23)], the conductance will be reduced. Mélin and Bourgeois extended the de Jong–Beenakker theory to a non-($Z=0$) barrier.[25] They showed that in case of high-Z interfaces, the effect of the Fermi surface polarization is less effective on the conductance. A polarization of 15% in a junction with an $Z=1$ barrier will lead to a loss of conductance below 1%. Hence, we do not expect a large effect of weak polarization in Gd on the junction resistance.

IV. CONCLUSIONS

In this paper, we describe high-sensitivity transport measurements on Nb/Al/Gd/Al/Nb and Nb/Al/Y/Al/Nb, two different types of $S/N/S$ junctions. By comparing Gd-based junctions to Y-based junctions, where the former is less stable than the latter, we pointed out the specific resistive behavior of such junctions. We gave a comprehensive description of the resistive behavior in such $S/N/S$ junction by performing and analyzing $V(I)$ measurements, the Josephson effect, and resistance versus temperature and magnetic field measurements.

We showed that in the Gd case, transport measurements are essentially controlled by interface scattering, while in the Y case resistance comes essentially from the bulk. We demonstrated this by getting very good agreement between BTK theory and our data. This theory, describing Andreev reflection in the case of nonideal interface transparency, gives a good description of the temperature dependence of the resistance through high values of the parameter Z, the interfacial potential. An interesting phenomenon of increase of resistance at low temperature was observed and is well described by the BTK theory. In the case of high-resistance junctions, the resistance can drop up to a factor of 10 at low temperature. This behavior cannot be due to the ferromagnetism in Gd, since the spin polarization at the Fermi energy is too low in this compound.

On the other hand, the low interface resistance in Y-based junction cannot be fitted using this theory. In conclusion, we have shown that in any experiment on S/F systems involving Gd, contributions of the interfaces to transport properties and hence to proximity effect or any interaction between magnetism and superconductivity, can be dominant. Any interpretation of experimental results has to take this into account.

ACKNOWLEDGMENTS

We wish to acknowledge M.O. Ruault for TEM images, F. Lalu for RBS measurements, and valuable discussions with R. Mélin, T. Klapwijk, and R.C. Dynes.

*Present address : University of California San Diego, 9500 Gilman Drive, 92093-0319 La Jolla, CA.
Email: olivier@physics.ucsd.edu

[1] C. Strunk, C. Sürgers, U. Pashen, and H. von Löhneysen, Phys. Rev. B **49**, 4053 (1994).
[2] J. S. Jiang, D. Davidovitch, D. H. Reich, and C. L. Chien, Phys. Rev. Lett. **74**, 314 (1995).
[3] Th. Mühge, N. N. Garif'ianov, Y. N. Goryunov, G. G. Khaliullin, K. Westerholt, I. A. Garifullin, and H. Zabel, Phys. Rev. Lett. **77**, 1857 (1996).

[4] A $S/X/S$ junction is called a π junction when there is a π-phase shift between both superconducting sides of the junction. X can be an insulating layer with paramagnetic impurities or a ferromagnetic layer. Unconventional order parameter symetry in high-temperature superconductors can also lead to π coupling.
[5] V. T. Petrashov, V. N. Antonov, S. V. Maximov, and R. S. Shaikhaidarov, Pis'ma Zh. Éksp. Teor. Fiz. **59**, 551 (1994) [JETP Lett. **59**, 551 (1994)].
[6] M. D. Lawrence and N. Giordano, J. Phys.: Condens. Matter **11**, 1089 (1999).
[7] M. Giroud, H. Courtois, K. Hasselbach, D. Mailly, and B. Pannetier, Phys. Rev. B **58**, R11 872 (1998).
[8] R. J. Soulen, J. M. Byers, M. S. Osofsky, B. Nadgorny, T. Ambrose, S. F. Cheng, P. R. Broussard, C. T. Tanaka, J. Novak, J. S. Moodera, A. Barry, and J. M. D. Coey, Science **282**, 85 (1998).
[9] S. K. Upadhyay, A. Palasinami, R. N. Louie, and R. A. Buhrman, Phys. Rev. Lett. **81**, 3247 (1998).
[10] P. Gandit, O. Bourgeois, J. Lesueur, A. Sulpice, X. Grison, and J. Chaussy, Physica B **284**, 497 (2000).
[11] O. Bourgeois, P. Gandit, J. Lesueur, A. Sulpice, X. Grison, and J. Chaussy (unpublished).
[12] O. Bourgeois, Ph.D. Thesis, Université Joseph Fourier, Grenoble, France (1999).
[13] I. Žutić and O. T. Valls, Phys. Rev. B **60**, 6320 (1999); **61**, 1555 (2000).
[14] P. Dauguet, P. Gandit, and J. Chaussy, J. Appl. Phys. **79**, 5823 (1996).
[15] D. Douglas, J. Bucher, and L. Bloomfield, Phys. Rev. Lett. **68**, 1774 (1992).
[16] U. Pashen, C. Sürgers, and H. von Löhneysen, Z. Phys. B **90**, 289 (1993).
[17] A. Barone and G. Patterno, *Physics and Applications of the Josephson Effect* (Wiley, New York, 1982).
[18] M. Tinkham, *Introduction to Superconductivity* (Mc Graw-Hill, New York, 1996).
[19] A. Andreev, Pis'ma Zh. Éksp. Teor. Fiz. **19**, 1228 (1974) [JETP Lett. **19**, 1228 (1974)].
[20] G. Blonder, M. Tinkham, and T. Klapwijk, Phys. Rev. B **25**, 4515 (1982).
[21] P-G. de Gennes, *Superconductivity of Metals and Alloys* (W.A. Benjamin Inc., New York, 1966).
[22] M. Octavio, M. Tinkham, G. Blonder, and T. Klapwijk, Phys. Rev. B **27**, 6739 (1983).
[23] R. Meservey and P. Tedrow, Phys. Rep. **238**, 173 (1994), and references therein.
[24] M. de Jong and C. Beenakker, Phys. Rev. Lett. **74**, 1657 (1995).
[25] R. Mélin and O. Bourgeois, in *Quantum Physics at Mesoscopic Scale*, edited by C. Glatti, M. Sanquer, and J. Tran Thanh Van, Series Moriond Condensed Matter Physics (Editions Frontieres, France, 1999).
[26] J. Aarts, J. M. E. Geers, E. Bruck, A. A. Golubov, and R. Coehoorn, Phys. Rev. B **56**, 2779 (1997).